'94 KACC (1994. 10. 17 ~ 20)

FLEXIBLE ARM POSITIONING USING H_∞ CONTROL THEORY WITH OPTIMUM SENSOR LOCATION

Rijanto Estiko, Shinya Nishigaya, Antonio Moran and Minoru Hayase
Tokyo University of Agriculture and Technology
Koganei-shi, Tokyo 184, Japan

This paper is concerned with the positioning control of a flexible arm system using H_∞ control theory with optimum sensor location. Firstly, by virtue of the orthogonality of the flexible modes of the flexible arm a reduced order model of the distributed parameter system (DPS) representing the arm has been formulated. The dynamical coupling between the flexible arm and DC motor has been considered to formulate an arm-motor composite model. In order to achieve precise positioning with vibration attenuation, sensors have been optimally located. Finally, a robust H_∞ controller was designed and the performance of the positioning system has been analyzed.
Keywords: DPS,Optimum sensor location, H_∞ controller.

1 Introduction

The demands for increased robot accuracy and high speed coupled with energy saving and large workspace requirements necessitate the evaluation of robot flexibility. Meanwhile, there has been many research on analysis and control of flexible structures, modeling and control of flexible arms has become one specialized field in this area. Modeling of flexible arms can be done by several methods : spring-mass vibration model, finite element method(FEM) model, and distributed parameter system (DPS) model. DPS models may properly represent the dynamics of the flexible arm and many results have been reported concerning this modeling method. However, most of these papers neglect the dynamics of the motor which drives and controls the flexible arm. Since the servo motor has limited capacity and is affected by the dynamics of the flexible arm, it is necessary to include the dynamics of the motor to formulate motor-arm composite models. In this sense this paper analyzes the modeling and control of flexible arms including the motor dynamics. The modeling of the flexible arm has been done considering a distributed parameter system model with reduced order.

It is known that certain performance goals can not be achieved through feedback control regardless of the control law used if certain structural conditions, such as observability, are not properly satisfied. In the case of flexible robot arm, rotational angle can be detected by using a potentiometer attached to the hub. The position of the tip of the flexible arm is composed by the rotational angle of the hub and the deflextion of the arm due to vibration. This vibration can be detected using strain gauge. Here, the optimum location of the strain gauge is determined by maximizing a Performance Index defined in terms of the energy of the measured signals which is related to the size of the observability gramian.

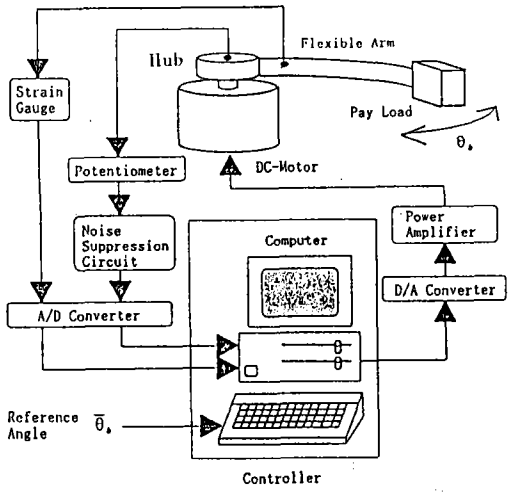

Figure 1: Structure of the experimental flexible arm and control system

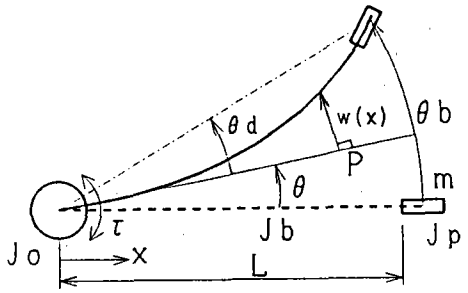

Figure 2: Theoretical model of slewing flexible arm

2 Modeling

2.1 Slewing Arm Equation

Figure 1 shows the structure of the experimental flexible arm and control system . Figure 2 shows the theoretical model. Hamilton's Principle can be utilized to obtain the linear equations of motion and boundary conditions of the flexible robot arm with torque actuation at the hub [1]. This principle is a kind of Variance Principle that can be formulated as:

$$\int_{t_1}^{t_2} \delta(T - V + W)dt \equiv 0 \qquad (1)$$

with δ denotes the variance, and T, V, W are kinetics energy, potential energy, and virtual work done by external forces, respectively.

In developing the equations of motion and natural boundary conditions the following assumptions have been made:
1. The arm is uniform, the deflection is small and only elastic deformation occurs.
2. The arm has high axial stiffness and flexibility only toward horizontal forces.
3. Local rotational moment and shear deformations are neglected (Eule-Bernoulli beam theory).
4. Viscousity of the air, internal friction of the arm and nonlinearity of the servo mechanism are neglectible.

By neglecting terms of second degree and higher, the integro-partial differential equations for the slewing arm motion and natural boundary conditions are obtained as follows
Equations of the slewing arm motion :

$$J_r\,\ddot{\theta}(t) + \rho A \int_0^L x\,w_{tt}(x,t)\,dx + m L\,\ddot{w}(L,t) = \tau(t) \qquad (2)$$

$$E I\,w_{xxxx}(x,t) + \rho A\,w_{tt}(x,t) = -\rho A\,x\,\ddot{\theta}(t) \qquad (3)$$

Natural boundary conditions :

$$w_{xx}(L,t) = 0 \qquad (4)$$

$$E I\,w_{xxx}(L,t) = m L\,\ddot{\theta}(t) + \ddot{w}(L,t) \qquad (5)$$

where the suffix x and t refer to partial derivatives respect to position x and time t, respectively.
Since the arm is constrained at $x = 0$, then the following geometric boundary condition is obtained :

$$w(0,t) = w_x(0,t) = 0 \qquad (6)$$

$\theta[rad]$ is the rotational angle of the hub, and the deflextion of a point P at $x[m]$ from the hub is represented by $w(x,t)[m]$. $\rho[kg/m^3]$, $A[m^2]$, $E[N/m^2]$, $I[m^4]$, $L[m]$ denote density, sectional area, Young's modulus, second moment of area and length, respectively. $J_o[kg \cdot m^2]$ is the moment of inertia of the hub including that of DC motor, $m[kg]$ is the mass of the pay load. And $J_r[kg \cdot m^2]$ is total moment inertia of the hub-arm-pay load system which can be calculated as

$$J_r = J_o + \rho A L^3/3 + mL^2 \qquad (7)$$

2.2 Unconstrained Mode Expansion

2.2.1 Solution of free motion equations

To solve the slewing arm equations, firstly $\tau(t) = 0$ is set to make a homogenuous integro-patial differential equation and to solve it by unconstrained mode expansion. The unconstrained mode expansion is defined as the natural motion obtained in the absence of all external influences. The structure as a whole is allowed to vibrate and the solution involves inertia properties of both the rigid and flexible parts.

Using the classical method of separation of variables

$$w(x,t) = \phi(x)\,q(t); \qquad \theta(t) = \eta(t) + p\,q(t) \qquad (8)$$

and substituting these equations in Eq.(4) and by assuming that:

$$J_r\,p + \rho A \int_0^L x\phi(x)dx + mL\phi(L) = 0 \qquad (9)$$

then the following equation is obtained

$$J r\,\ddot{\eta}(t) = 0 \qquad (10)$$

On the other hand, combining Eq.(8) and Eq.(5) the following two independent equations related to time t and location x are obtained

$$\ddot{q}(t) + \omega^2\,q(t) = 0 \qquad (11)$$

$$\phi''''(x) - \frac{\rho A}{E I}\omega^2\,[p\,x + \phi(x)] = 0 \qquad (12)$$

where ω is a positive constant.
Also, combining Eq.(8) and the boundary conditions equations the following conditions are obtained

$$\phi(0) = \phi'(0) = \phi''(L) = 0; \quad \phi'''(L) = -\frac{m}{E I}\omega^2\,[p\,L + \phi(L)] \qquad (13)$$

Morcover, from Eq.(4),(9),(12)

$$p = -\frac{E I}{J_o\,\omega^2}\phi''(0) \qquad (14)$$

To simplify the analysis, introduce the transformation of variables $\psi(x) = \phi(x) + p\,x$, so that Eq.(13) becomes

$$\psi''''(x) - \beta^4\,\psi(x) = 0 \qquad (15)$$

where $\beta^4 = \dfrac{\rho A \omega^2}{E I}$. Eq.(15) expresses an eigen-value problem with β as eigen-value and $\psi(x)$ as eigen-function. The general solution for Eq.(15) has the form

$$\psi(x) = C_1 Cos(\beta x) + C_2 Sin(\beta x) + C_3 Cosh(\beta x) + C_4 Sinh(\beta x) \qquad (16)$$

Coefficients C_1, C_2, C_3, C_4 can be obtained from the following matrix equation

$$\begin{bmatrix} 1 & 0 & 1 & 0 \\ -\gamma\beta^2 & \beta & \gamma\beta^2 & \beta \\ -\beta^2 c^* & -\beta^2 s^* & \beta^2 ch^* & \beta^2 sh^* \\ \beta^3 s^* + \alpha c^* & -\beta^3 c^* + \alpha s^* & \beta^3 sh^* + \alpha ch^* & \beta^3 + \alpha sh^* \end{bmatrix} \begin{bmatrix} C_1 \\ C_2 \\ C_3 \\ C_4 \end{bmatrix} = \begin{bmatrix} 0 \\ 0 \\ 0 \\ 0 \end{bmatrix}$$

where : $s^* = sin(\beta L)$, $c^* = cos(\beta L)$,
$sh^* = sinh(\beta L)$, $ch^* = cosh(\beta L), \alpha = \frac{m\Omega^2}{EI}$, $\gamma = \frac{EI}{J_o\Omega^2}$

For this matrix equation to have a solution other than the trivial one, the following equation must hold

$$\begin{aligned} &\{1 + cos\beta L cosh\beta L + \\ &(\frac{\rho A}{J_o}\beta^{-3} - \frac{m}{\rho A}\beta) sin\beta L cosh\beta L - sinh\beta L cos\beta L) \\ &+2\frac{m}{J_o}\beta^{-2} sin\beta L sinh\beta L\} = 0 \end{aligned} \qquad (18)$$

Equation (18) has an infinite number of solutions for β. The coefficient C_1, C_2, C_3, C_4 are not independent from each other so that for any β_i, C_2, C_3, C_4 can be expressed as depending on $C_1 = C_i$ which is determined in order to normalize the solution. The above eigen-value problem has the solution

$$\begin{aligned} \phi(x) &= \{cos\beta x - \{\frac{cos\beta L + cosh\beta L - 2\frac{\rho A}{J_o}\beta^{-3} sinh\beta L}{sin\beta L + sinh\beta L}\} sin\beta x \\ &- cosh\beta x + \{\frac{cos\beta L + cosh\beta L + 2\frac{\rho A}{J_o}\beta^{-3} sin\beta L}{sin\beta L + sinh\beta L}\} sinh\beta x \\ &- 2\frac{\rho A}{J_o}\beta^{-2} x\} C_i \end{aligned} \qquad (19)$$

and the solution for $w(x,t)$ and $\theta(t)$ are expanded as follows:

$$\theta(t) = \eta(t) + \sum_{i=1}^{\infty} p_i\,q_i(t); \quad w(x,t) = \sum_{i=1}^{\infty} \phi_i(x)\,q_i(t) \qquad (20)$$

where, $x \in [0, L], t \geq 0$.

2.2.2 Orthogonality of eigen-value problem and solution of forced motion equations

Assuming that there are two different solutions $\phi_i(x), \phi_j(x)$ of the eigen-value problem stated by Eq.(12)

$$E\,I\,\phi_i''''(x) = \rho\,A\,\omega_i^2\,[\phi_i(x) + p_i\,x] \quad (21)$$
$$E\,I\,\phi_j''''(x) = \rho\,A\,\omega_j^2\,[\phi_j(x) + p_j\,x] \quad (22)$$

The orthogonality conditions to be satisfied by the different solutions of the problem are obtained as follow
From Eq.(21) :

$$\int_0^L EI\phi_j(x)\phi_i''''(x)dx = \rho A\omega_i^2 \int_0^L \phi_j(x)\phi_i(x)dx + \rho A\omega_i^2 \int_0^L \phi_j(x)p_i x dx \quad (23)$$

From Eq.(22) :

$$\int_0^L EI\phi_i(x)\phi_j''''(x)dx = \rho A\omega_j^2 \int_0^L \phi_i(x)\phi_j(x)dx + \rho A\omega_j^2 \int_0^L \phi_i(x)p_j x dx \quad (24)$$

On substracting Eq.(23) from (24), applying boundary conditions, and substituting Eq.(9) the following equation is obtained

$$\int_0^L \rho A\phi_i(x)\phi_j(x)dx + m\phi_i(L)\phi_j(L) - J_r p_i p_j = 0, i \neq j \quad (25)$$

On the other hand, by applying boundary conditions Eq.(23) can be modified to

$$\int_0^L EI\phi_j''(x)\phi_i''(x)dx = \omega_i^2[\int_0^L \rho A\phi_j(x)\phi_i(x)dx + m\phi_j(L)\phi_i(L) - J_r p_i p_j] \quad (26)$$

By normalizing the eigen-modes of the flexible arm, the following relations are obtained :

$$\int_0^L \rho A\phi_i(x)\phi_j(x)dx + m\phi_i(L)\phi_j(L) - J_r p_i p_j = \delta_{ij} \quad (27)$$
$$\int_0^L EI\phi_j''(x)\phi_i''(x)dx = \omega_i^2\delta_{ij} \quad (28)$$

where, $i, j = 1, 2, \ldots$, and δ_{ij} denotes Kronecker delta.
These properties of orthogonality are used to solve the forced motion equations . Substituting Eq.(27),(28) in to Eq.(4) :

$$J_r\ddot{\eta} = \tau(t) \quad (29)$$

then from Eq.(5)

$$\ddot{q}_i(t) + \omega_i^2 q_i(t) = \kappa_i \tau(t) \quad (30)$$

where $\kappa_i = \dfrac{[p_j + \frac{m\phi_j(L)}{J_r}]}{\sum_{i=1}^{\infty}\{\delta_{ij} - m\phi_j(L)[p_i L + \phi_i(L)]\}}$

2.3 State space equations and output equations

The above eigen-value analysis results in a second order differential equation of the form shown in Eq.(20). Since the model will be used to design a controller, the degree of the the model should be low enough because of the limitation in the sampling time of control. By virtue of the orthogonality of each mode, the model can be reduced to any degree, for example order 2, including rigid mode and the first elastic mode.

Taking into account the effects of viscousity, the second order differential equations become

$$J_r\ddot{\eta} + D\dot{\eta} = \tau(t) \quad (31)$$
$$\ddot{q}_i + 2\zeta_i\omega_i\dot{q}_i + \omega_i^2 q_i = b_i\tau(t), \quad i = 1. \quad (32)$$

The arm is rotated by a DC motor, so the motor dynamics should be incorporated into the structural equations of the model. Deriving the equations of motion (2), (3), the moment of inertia of the motor was included, but for the reason of analysis the counter-electromotive force (emf) was not taken into account. Having obtained the mode function, the emf is included into the dynamic equations described by Eq.31, 32. The voltage supplied to the motor u, the motor torque τ, and the emf are related by the following equation :

$$\tau = \frac{K_t}{Ra}[u - K_e\dot{\theta}] \quad (33)$$

where K_t, Ra, K_e, $\dot{\theta}$ are torque constant, internal resistance, emf constant, and angular velocity of the motor shaft.
By combining Eq.(31),(32),(33), and arranging them properly the following state space equation is obtained

$$\dot{\mathbf{x}} = A\mathbf{x} + Bu \quad (34)$$

where $\mathbf{x} = [\dot{\eta}\ \eta\ \dot{q}_1\ q_1]^T := [x_1\ x_2\ x_3\ x_4]^T$ is the state vector and q_1 represents the first vibrational mode of the arm. A, B have the size of 4×4, and 4×1 respectively. The detailed description of the state-space equation will be shown latter in section 4.

The experimental setting has 2 sensors, potentiometer and strain gauge. The output equation can be described as

$$y = \begin{bmatrix} y_1 \\ y_2 \end{bmatrix} = \begin{bmatrix} 0 & K_{pm} & 0 & K_{pm}\,p_1 \\ 0 & 0 & 0 & K_{sg}\,\mu(x) \end{bmatrix} \begin{bmatrix} \dot{\eta} \\ \eta \\ \dot{q}_1 \\ q_1 \end{bmatrix} \quad (35)$$

$$y = Cx \quad (36)$$

where y_1 denotes the output from the potentiometer and y_2 denotes that of strain gauge. K_{pm}, K_{sg} are the constant of the potentiometer and strain gauge respectively. The coefficient $\mu(x)$ is defined as

$$\mu(x) = -\frac{T_h}{2}\frac{d^2\phi(x)}{dx^2} \quad (37)$$

Where T_h is the thickness of the arm. The procedure to determine the optimal location of the strain gauge will be presented in section 3.

2.4 Modeling and Experimental Results

Figure 3 shows the first 3 flexible modes shapes obtained by the theoretical analysis. Figure 4 compares the frequency responses of the experimental and theoretical results. The resonant frequency of the first flexible mode of the theoretical results is the same as that of the experimental ones. It can be noted that theoretical and experimental responses are close to each other for the analyzed frequency range. This good agreement between both responses verifies the validity of the theoretical model developed in this paper.
Table 1 shows the values of the parameter of the model.

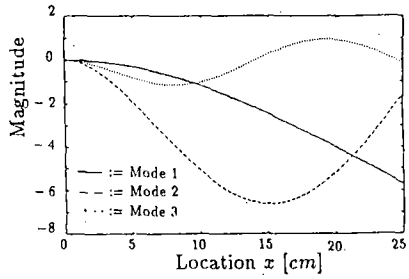

Figure 3: Modes shapes

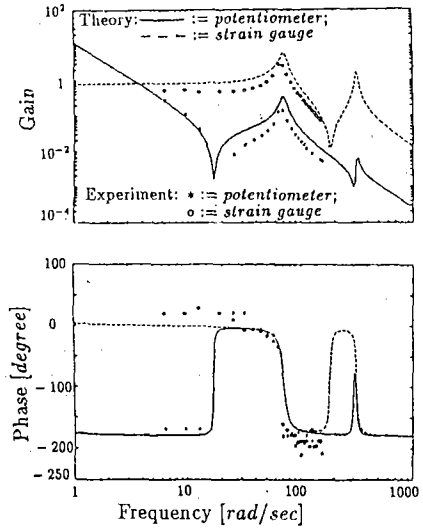

Figure 4: Frequency response

Table 1 *Motor – Arm and Pay Load parameters*

Parameter	Value	Unit
Arm-Payload		
E	1.96×10^{11}	N/m
I	2.08×10^{-12}	m^4
A	25×10^{-6}	m^2
L	0.25	m
T	1×10^{-3}	m
ρ	10.667×10^{3}	Kg-m^{-3}
Jb	1.667×10^{-3}	Kg-m^2
m	0.2	Kg
Jp	10.971×10^{-3}	Kg-m^2
Jo	1×10^{-3}	Kg-m^2
Motor-hub		
Ra	1.3	Ω
Kt	0.0735	N · m/A
Ke	0.0735	V · s/rad
D	0.0001	N · m · s/rad
Kpm	0.8185	V/rad
Kpa	10	-
Ksg	2500	V

3 Optimum Sensor Location

As mentioned before, the experimental setting has a potentiometer and a strain gauge as sensors. Since the location of the potentiometer is determined structurely, the location of the strain gauge will be optimally determined. The determination of the optimum strain gauge location is carried out independently of the design of the control law. Several strategies may be formulated to determined the optimal location of the strain gauge. Two are the most common methods: maximization of the energy of the output signals(measured signals) and filtering techniques for the optimal estimation of the state variables of the flexible arm model. In this paper, the first mentioned method has been considered.

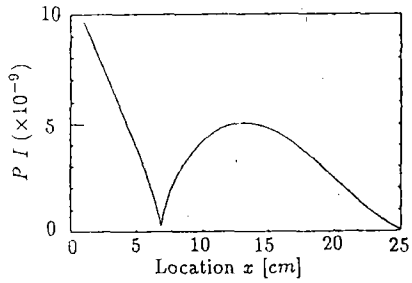

Figure 5: Performance Index of sensor location

The objective is to find the matrix C in Eq.(36) that maximizes the energy of output $y(t)$. If the system is released from the initial state $x(t_0)$, then energy of the output vector can be expressed as

$$E = trace[\int_0^\infty y^T(t)y(t)dt] = trace\{x_0^T Q x_0\} \qquad (38)$$

where Q is the observability gramian. The gramian Q satisfies the Lyapunov equation

$$A^T Q + QA + C^T C = 0 \qquad (39)$$

The Performace Index PI for location of strain gauge is chosen so that the norm of the observability gramian be as large as posible and its individual eigen-values are large [3].

$$PI = \left(\sum_{i=1}^{2N} \lambda_i\right)\left(\prod_{i=1}^{2N} \lambda_i\right)^{\frac{1}{2N}} \qquad (40)$$

where λ_i denotes the eigen-value of the observability gramian Q. Fig.5 shows how PI changes as x varies from 0 to 25 cm. It is clear that the strain gauge is better located near the hub.

4 H_∞ control design

4.1 H_∞ control theory

In this study, the DGKF H_∞ control theory [4] was adopted to design a controller for the flexible arm. Figure 6 shows the standard set-up of the H_∞ control problem. In this figure u, y, w, and z are vector-valued signals: u is the control input; y is the measured output; w is the exogenous input, and z is the evaluation output to be controlled. The transfer matrices G and K are real-rational and represent the generalized plant and the controller, respectively. The *standard problem* is to find a real-rational K that minimizes the H_∞-norm of the transfer matrix from w to z ($:= T_{zw}$) under the constraint that K stabilizes G [5]. In the frequency domain the H_∞ norm of the transfer matrix T_{zw} is defined as:

$$\|T_{zw}\|_\infty := \sup_\omega \sigma_{max}[T_{zw}]; \quad (\sigma_{max} := maximum\ singular\ value) \qquad (41)$$

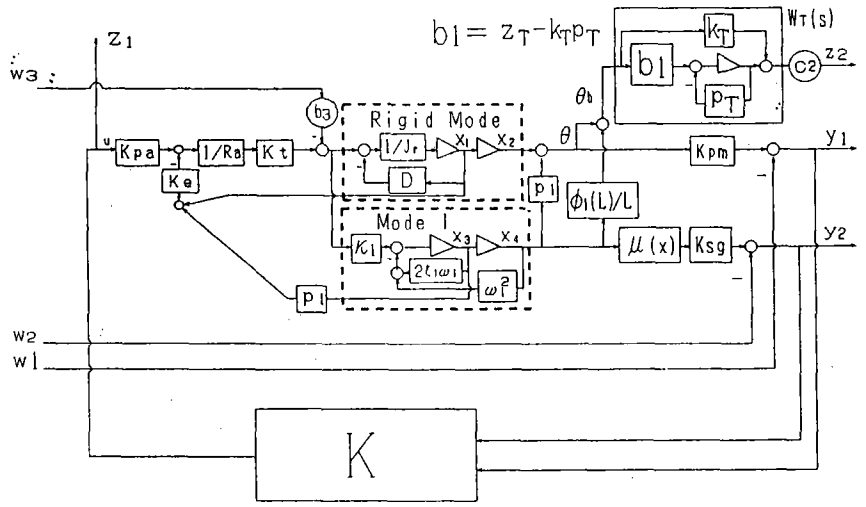

$$\begin{bmatrix} \dot{x}_1 \\ \dot{x}_2 \\ \dot{x}_3 \\ \dot{x}_4 \\ \dot{x}_5 \\ \hline y_1 \\ \underline{y_2} \\ z_1 \\ z_2 \end{bmatrix} = \left[\begin{array}{ccccc|ccc} -\frac{[DR_a + K_eK_t]}{R_aJ_r} & 0 & -\frac{K_eP_1K_t}{R_aJ_r} & 0 & 0 & \frac{K_{pa}K_t}{R_aJ_r} & 0 & 0 & -\frac{b_3}{J_r} \\ 1 & 0 & 0 & 0 & 0 & 0 & 0 & 0 & 0 \\ -\frac{\kappa_1K_eK_t}{R_a} & 0 & -[2\zeta_1\omega_1 + \frac{\kappa_1K_eP_1K_t}{R_a}] & -\omega_1^2 & 0 & \frac{\kappa_1K_{pa}K_t}{R_a} & 0 & 0 & -b_3\kappa_1 \\ 0 & 0 & 1 & 0 & 0 & 0 & 0 & 0 & 0 \\ 0 & b_1 & 0 & b_1g_{11} & -p_T & 0 & 0 & 0 & 0 \\ \hline 0 & K_{pm} & 0 & K_{pm}P_1 & 0 & 0 & -1 & 0 & 0 \\ 0 & 0 & 0 & -K_{sg}\mu(x) & 0 & 0 & 0 & -1 & 0 \\ \hline 0 & 0 & 0 & 0 & 0 & 1 & 0 & 0 & 0 \\ 0 & c_2k_T & 0 & c_2k_Tg_{11} & c_2 & 0 & 0 & 0 & 0 \end{array}\right] \begin{bmatrix} x_1 \\ x_2 \\ x_3 \\ x_4 \\ x_5 \\ \hline u \\ \underline{w_1} \\ w_2 \\ w_3 \end{bmatrix}$$

Figure 7: Block diagram of the closed loop and generalized plant matrix

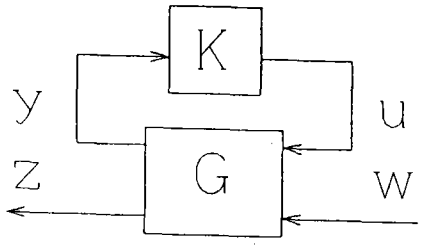

Figure 6: H_∞ Standard Problem

Many control problems such as: disturbance attenuation, robust stabilization, tracking problem, model matching problem can be transformed to the standard H_∞ control problem for which *the optimal criterion* to design the controller is

$$\|\gamma T_{zw}\|_\infty < 1 \tag{42}$$

The control design specifications are incorporated in the design procedure by introducing frequency-dependent weighting functions. By combining the nominal plant and the weighting functions the *generalized plant* can be formulated as:

$$\dot{\mathbf{x}} = -A\mathbf{x} + B_1u + B_2w \tag{43}$$

$$y = C_1\mathbf{x} + D_{11}u + D_{12}w \tag{44}$$

$$z = C_2\mathbf{x} + D_{21}u + D_{22}w \tag{45}$$

The following assumptions are made on the generalized plant in order to directly apply the DGKF design procedure of H_∞ controllers:

(0).$D_{11} = 0$, and $D_{22} = 0$

(1).$(-A, B_1)$ is stabilizable and $(C_1, -A)$ is detectable.

(2).$(-A, B_2)$ is stabilizable and $(C_2, -A)$ is detectable.

(3).$D_{21}^T[C_2 \;\; D_{21}] = [0 \;\; I]$; $\begin{bmatrix} B_2 \\ D_{12} \end{bmatrix} D_{12}^T = \begin{bmatrix} 0 \\ I \end{bmatrix}$

The H_∞ controller can be constructed by solving the following two Algebraic Riccati Equations:

$$X[B_1B_1^T - \gamma^2 B_2B_2^T]X + A^TX + XA - C_2^TC_2 = 0 \quad (46)$$
$$Y[C_1^TC_1 - \gamma^2 C_2^TC_2]Y + AY + YA^T - B_2B_2^T = 0 \quad (47)$$

The Riccati solutions X and Y should satisfy:
1). $X \geq 0$; 2). $Y \geq 0$
3). $\gamma^2 \rho\Big(XY\Big) < 1$; $\rho\Big(XY\Big) :=$ *spectral radius of* XY

Then, the controller which satisfies the H_∞ control criterion $\|\gamma T_{zw}\|_\infty < 1$ is:

$$\dot{\hat{x}} = -\hat{A}\hat{x} + \hat{B}_2 y \quad (48)$$
$$u = -\hat{C}_2\hat{x} \quad (49)$$
$$\hat{A} = A + [B_1B_1^T - \gamma^2 B_2B_2^T]X + ZYC_1^TC_1 \quad (50)$$
$$\hat{B}_2 = ZYC_1^T;\ \hat{C}_2 = B_1^TX;\ Z = [I - \gamma^2 YX]^{-1} \quad (51)$$

4.2 H_∞ controller design

To synthesize the controller a nominal plant considering the rigid and first elastic modes was considered.
The design specifications are :
1). To design a controller of reduced order model which stabilizes the real plant.
2). The steady state error converges to zero when a step reference is applied.
To achieve these design specifications a regulator control system shown in Fig.7 was constructed. θ_b is the angular position of the tip of the arm. w_1, w_2 are both measurement noises, and w_3 is Coulomb friction disturbance. Assuming that the Coulomb friction is small enough, the constant weight b_3 is set to be small. The step reference is applied at the gate of w_1. The parameters of the frequency dependent weighting function $W_T(s)$ are chosen in order to satisfy the design specifications. $W_T(s)$ has the form

$$W_T(s) = k_T \frac{s + z_T}{s + p_T} \quad (52)$$

The steady state error is related to the sensitivity function $S(s)$, and the robust stability to the complement sensitivity function $T(s)$

$$S(s) = \frac{r^*(s) - \theta_b(s)}{r^*(s)};\quad T(s) = \frac{\theta_b(s)}{r^*(s)};\quad \left(r^*(s) = \frac{r(s)}{K_{pm}}\right) \quad (53)$$

If γ is set to be $\gamma = 1$, then the design specifications can be expressed in the following criterion:

$$\|W_T(s)T(s)\|_\infty < 1 \quad (54)$$

4.3 Simulation results and considerations

The weighting function $W_T(s)$ was selected to satisfy :

$$|W_T(s)| \geq \sigma_{max}[\frac{\Delta_A(s)}{P_a(s)}];\quad P_a(s) = \frac{\theta_b(s)}{\tau(s)} \quad (55)$$

where $\Delta_A(s)$ is the transfer functions of the unmodeled higher flexible modes. This weighting function and the design specifications are shown in Fig.8. The singular values of the design criterion $T_{zw}(s)$ are shown in Fig.9 and the response of the tip of the arm θ_b for a step reference is shown in Fig.10. It can be noted that the tip of the arm is able to track the step reference input with zero steady-state error.

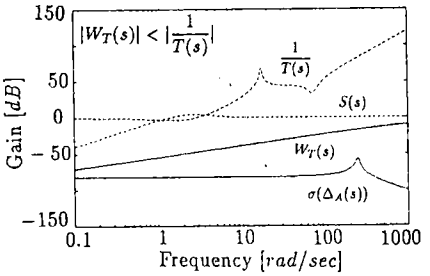

Figure 8: Weighting function and design specifications

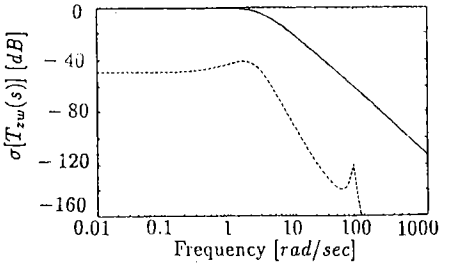

Figure 9: Singular value of $T_{zw}(s)$

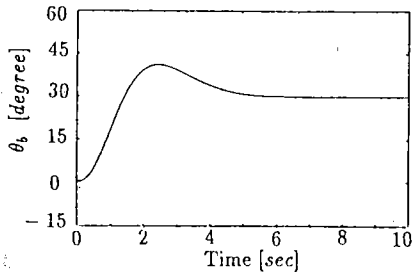

Figure 10: Step response of the real plant with disturbances

5 Conclusions

The modeling of a flexible arm including motor dynamics has been formulated and verified experimentally. The model was formulated based on the Distributed Parameter System method decoupling the rigid and flexible modes of the arm. A potentiometer and a strain gauge were used to monitor and control the motion of the flexible arm. The location of the strain gauge has been optimally determined by maximizing a performance index defined in terms of the energy of the measured(output) signals. An H_∞ feedback controller has been designed and the tracking performance and robustness properties of the closed loop system have been verified.

References

[1] H.Kanoh,"Distributed Parameter Models of Flexible Robot Arms", Japan Robot Society Journal,(in Japanese), Vol.6, No.5, 1988

[2] L.Meirovitch, "Elements of Vibration Analysis", McGraw-Hill, 1975

[3] Alexsander Hac and Linghua Liu, "Sensor and Actuator Location in Motion Control of Flexible Structure", The 1st International Conf. on Motion and Vibration Control, 1992

[4] Doyle J.C., Glover K., Khargonekar P., and Francis B., "State-Space Solutions to Standard H_2 and H_∞ Control Problems", IEEE Trans. on Automatic Control, Vol.34, No.8, 1989.

[5] B.A.Francis, "A course in H_∞ control theory",(Lecture Notes in Control and Information Sciences, Vol.88). New York: Springer-Verlag, 1987